Von Herzen, R. P., Robinson, P. T., et al., 1991
Proceedings of the Ocean Drilling Program, Scientific Results, Vol. 118

6. GEOCHEMISTRY AND ISOTOPIC COMPOSITION OF GABBROS FROM LAYER 3 OF THE INDIAN OCEAN CRUST, HOLE 735B[1]

P. D. Kempton,[2,3] C. J. Hawkesworth,[2] and M. Fowler[3]

ABSTRACT

Gabbros drilled from the shallow (720 m) east wall of the Atlantis II transform on the Southwest Indian Ridge (SWIR; 32°43.40′, 57°16.00′) provide the most complete record of the stratigraphy and composition of the oceanic lower crust recovered from the ocean basins to date. Lithologies recovered include gabbro, olivine gabbro, troctolite, trondhjemite, and unusual iron-titanium (FeTi) oxide-rich gabbro containing up to 30% FeTi oxides. The plutonic rock sequence represents a tholeiitic fractionation trend ranging from primitive magmas having Mg numbers of 67 to 69 that fractionated troctolites, to highly evolved liquids that crystallized two-pyroxene, FeTi oxide-rich gabbros and, ultimately, trondhjemite.

Isotopic compositions of unaltered Leg 118 gabbros are distinct from Indian Ocean mid-ocean ridge basalts (MORB) in having higher $^{143}Nd/^{144}Nd$ (0.51301–0.51319) and lower $^{206}Pb/^{204}Pb$ values (17.35–17.67); $^{87}Sr/^{86}Sr$ values (0.7025–0.7030) overlap those of SWIR basalts, but are generally lower than MORBs from the Southeast Indian Ridge or the Rodrigues Triple Junction. More than one magma composition may have been introduced into the magma chamber during its crystallization history, as suggested by the higher $^{87}Sr/^{86}Sr$, $^{206}Pb/^{204}Pb$, and lower $^{143}Nd/^{144}Nd$ values of chromium-rich olivine gabbros from the bottom of Hole 735B.

Whole-rock gabbro and plagioclase mineral separate $^{87}Sr/^{86}Sr$ values are uniformly low (0.7027–0.7030), irrespective of alteration and deformation. By contrast, $^{87}Sr/^{86}Sr$ values for clinopyroxene (0.7025–0.7039) in the upper half of Hole 735B are higher than coexisting plagioclase and reflect extensive replacement of clinopyroxene by amphibole. Hydrothermal veins and breccias have elevated $^{87}Sr/^{86}Sr$ values (0.7029–0.7035) and indicate enhanced local introduction of seawater strontium. Oxygen- and hydrogen-isotope results show that secondary amphiboles have uniform δD values of −49 to −54‰ and felsic hydrothermal veins range from −46 to −77‰. Oxygen-isotope data for secondary amphibole and visibly altered gabbros range to low values (+1.0–+5.5‰), and O-isotope disequilibrium between coexisting pyroxene and plagioclase pairs from throughout the stratigraphic column indicates that seawater interacted with much of the gabbro section, but at relatively low water/rock ratios. This is consistent with the persistence of low $^{87}Sr/^{86}Sr$ values, even in gabbros that were extensively deformed and altered.

INTRODUCTION

Isotope and trace-element variations in oceanic basalts are well established and widely used for speculating about the causes of chemical heterogeneities in the Earth's mantle and on the spatial relations of different reservoirs in models of mantle convection. However, such arguments are poorly constrained because the scale of the heterogeneities sampled at oceanic spreading centers, particularly within the lower crust, is not well known. In large part, there are simply too few data regarding the nature of magma chambers in this environment; magma chambers have been invoked beneath some mid-ocean ridges (MOR) (Macdonald et al., 1988), and ruled out beneath portions of others (Whitehead et al., 1954). In addition, there are still many unknowns with respect to magma interaction and crystallization processes in MOR magma chambers as well. Previous models of the structure and composition of the oceanic crust have relied heavily on data from ophiolites, but there is increasing concern that these rocks were generated in subduction-related environments and may not be directly applicable to models of crust generation at MORs.

Nevertheless, the composition of the total ocean crustal section is central to any investigation of global elemental fluxes; yet, present sampling of the ocean crust has been limited to the upper kilometer or less. Only in DSDP Hole 504B was a continuous sampling recovered through pillow basalts into the sheeted dikes of layer 2. This leaves the composition of the plutonic rocks of layer 3—which may constitute more than 50% of the ocean crust—virtually unknown. Scientists think that subducted crust contributes both to island- and back-arc magmatism, and to the development of chemical heterogeneities in the upper mantle. Thus, models for crust-mantle fluxes remain difficult to evaluate without better data for the lower oceanic crust and, in particular, about the extent to which this crust has been affected by hydrothermal alteration.

During Leg 118, scientists successfully recovered nearly 435 m of gabbro from the 500-m Hole 735B. This represents a phenomenal average recovery of 87%, and is the first such continuous section of oceanic layer 3 from the ocean basins. Thus, the objectives of this study are as follows:

1. To evaluate the composition of the lower oceanic crust,
2. To assess the isotopic heterogeneity of the gabbro parental magmas, and
3. To establish the isotopic effects and extent of hydrothermal alteration on oceanic layer 3.

GEOLOGIC SETTING

The gabbros in Hole 735B were drilled from the Atlantis II Fracture Zone, located on the Southwest Indian Ridge

---

[1] Von Herzen, R. P., Robinson, P. T., et al., 1991. *Proc. ODP, Sci. Results*, 118: College Station, TX (Ocean Drilling Program).

[2] Department of Earth Sciences, The Open University, Milton Keynes, MK7 6AA, United Kingdom.

[3] NERC Isotope Geology Laboratory, Keyworth, NG12 5GG, United Kingdom.

(SWIR) in the Indian Ocean. The north-south oriented Atlantis II Fracture Zone is one of a series of major transform faults offsetting the slow (0.8 cm/yr) spreading SWIR. The fracture zone crosses the ridge at approximately 57°E, and is approximately 5 to 6 km deep, about 30 to 40 km wide, and 210 km long. Site 735 is located on a shallow platform in about 700 m of water on the east rim of the fracture zone. The platform at Site 735 is about 5 km long in a north-south direction and 2 km wide. This platform has a flat surface, suggesting that it is a wave-cut feature. Based on the crust's position within the pattern of magnetic anomalies, crustal age is estimated as 12 Ma.

ANALYTICAL TECHNIQUES

Eighty-five samples were selected from the 435-m core recovered from Hole 735B. Standard thin sections were prepared for all 85 samples; 25 were then selected for microprobe studies. Analyses of the radiogenic isotopes strontium, neodymium, and lead and/or the stable isotopes, hydrogen and oxygen, were performed with whole-rock and/or mineral separates from 33 of these samples. Mineral separates for isotopic analyses were hand-picked from crushed and sieved split halves of the whole-rock sample. The mineral separates and whole-rock samples were then cleaned ultrasonically in 2.5 molar HCl to remove any surface contamination acquired through drilling, rinsed in distilled water, and hand-picked again in alcohol to ensure the purity of the sample. Samples then were crushed in an agate mortar.

Isotopic results are presented in Table 1. All Sr, Nd, and Pb isotope analyses were performed with a Finnegan MAT 261 multicollector mass spectrometer at the Open University. Sr and Nd were separated by standard one- and two-column cation exchange techniques and run as the metal species on single (Ta) and double (Re + Ta) filament assemblies, respectively. Pb was separated using columns prepared from PVP disposable pipette tips fitted with a 2-mm-diameter teflon plug and three to four drops of Dowex 1 × 8, 200- to 400-mesh anion exchange resin; completely new columns were prepared for each sample to minimize the Pb blank. Blanks for Pb, Sr, and Nd were less than 1.5, 5, and 1 ng, respectively. The average $^{87}Sr/^{86}Sr$ ratio for the NBS987 standard was 0.71023 ± 3, and the average $^{143}Nd/^{144}Nd$ for the Johnson Matthey Nd standard was 0.51191 ± 3. $^{87}Sr/^{86}Sr$ was normalized to $^{86}Sr/^{88}Sr = 0.1194$; $^{143}Nd/^{144}Nd$ was normalized to a value of $^{146}Nd/^{144}Nd = 0.7219$ and to an accepted $^{143}Nd/^{144}Nd$ value for the Johnson Matthey standard of 0.51184. Ratios of $^{18}O/^{16}O$ and D/H^+ and contents of H_2O^+ were determined by NERC Scientific Services at the Isotope Geology Centre (London, UK) and the Scottish University Research and Reactor Centre (East Kilbride, UK) and are represented as per mil (‰) deviations relative to standard mean ocean water (SMOW).

Major- and trace-element analyses of Leg 118 gabbros used here are those determined on board ship with a wave-length dispersive ARL 8420 X-ray fluorescence spectrometer (see Shipboard Scientific Party, 1989). Standard CIPW (Cross, Iddings, Pirsson, and Washington) norms were calculated from these data, assuming $Fe^{+2}/(Fe^{+3} + Fe^{+2}) = 0.85$. Mg numbers were calculated as $Mg/(Mg + Fe^{+2})*100$.

Major-element mineral compositions were performed at The Open University using a Cambridge Instruments Microscan 9 (M9) wave-length dispersive electron microprobe. Standard silicate analyses were performed in fully automated mode at an accelerating potential of 20 kV, a beam current of 30.5 nA, and a typical spot size of 10 to 15 μm. The instrument was calibrated daily using mineral standards: wollastonite (Si, Ca), rutile (Ti), metal (Cr, Mn, Ni), jadeite (Al, Na), fayalite (Fe), and forsterite (Mg). Consistency of the data was checked by analyzing an internal basaltic glass standard.

DESCRIPTION OF SAMPLES AND STRATIGRAPHIC SUMMARY

Samples recovered vary widely in degree of deformation, alteration, and primary mineralogy (Pl. 1), and the principle mineralogical and geochemical features, together with the six recognized lithologic units, are summarized in Figure 1. The mineralogic and petrographic characteristics of the specific samples analyzed for this study are summarized in Table 2. Rocks from the upper 40 m (Unit I) typically are highly deformed porphyroclastic to mylonitic metagabbros in which plagioclase porphyroclasts exhibit evidence for both high-temperature plastic deformation, as well as recrystallization into fine-grained neoblasts (Fig. 2). Clinopyroxene is also preserved as deformed porphyroclasts, but generally it is partially to completely replaced by amphibole (Fig. 3). Orthopyroxene occurs in this interval, but is generally replaced by talc + tremolite + Fe oxides. These rocks typically have low Mg numbers and normative anorthite contents, but are relatively enriched incompatible trace elements, particularly rubidium and zirconium (Fig. 4). Modal zirconium was observed in several samples from this unit.

Unit II is defined by a marked decrease in the degree of high-temperature plastic deformation and an increase in the variety of primary lithologies. The predominant lithology in Unit II is variably altered olivine gabbro having Mg numbers of 80 to 82, but the unit is interlayered with assemblages ranging from relatively evolved FeTi; oxide-rich gabbros to primitive troctolites. The upper boundary with Unit I is defined by a sharp decrease in the degree of deformation.

Unit III is composed of olivine gabbro having intervals of FeTi oxide gabbro. The olivine gabbro of this unit has a lower modal proportion of olivine and a higher proportion of orthopyroxene, making its primary mineralogy similar to that in Unit I, but the extent of deformation is more restricted, and much of the unit is undeformed. The gradational nature of the petrological data suggests that lithologic Units II and III are part of a continuous magmatic unit.

Unit IV consists of nearly 50 m of highly evolved, FeTi oxide-rich gabbros. These rocks are unusual in that they contain up to 30% modal FeTi oxide. They frequently contain

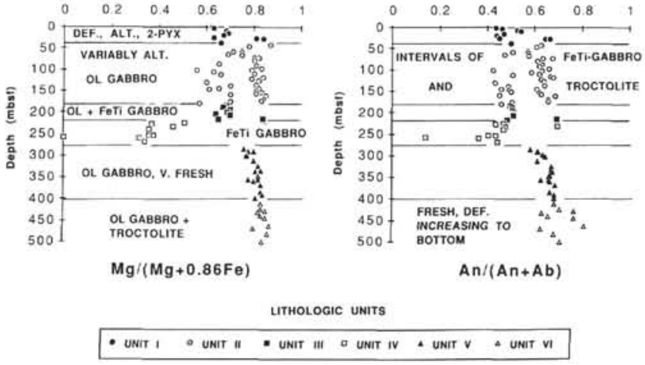

Figure 1. Summary of lithologic and geochemical variations of Leg 118 gabbros in terms of Mg number and normative plagioclase composition as a function of depth, measured in meters below the seafloor. Mg/(Mg+0.85Fe) and An/(An+Ab) are calculated from CIPW normative analyses of whole-rock XRF major-element data. Boundaries between the six units currently recognized are indicated by horizontal lines; see text for discussion.

Table 1. Sr-, Nd-, Pb-O-, and H- isotopes in Leg 118 gabbros.

Core, Section, Interval (cm)	Lithologic Unit	Depth	$^{87}Sr/^{86}Sr$	$^{143}Nd/^{144}Nd$	$^{206}Pb/^{204}Pb$	$^{207}Pb/^{204}Pb$	$^{208}Pb/^{204}Pb$	$\delta^{18}O$	H_2O (wt%)	δD
1D-2, 80-83(pl)	I	2	0.702792±16	0.513157±12	17.528± 1	15.558± 1	37.386± 2	+5.8		
1D-2, 80-83 (cpx)		2	0.703748±17	0.513181± 7				+5.2		
1D-2, 80-83 (wr)		2	0.702994±10		17.609± 1	15.485± 1	37.366± 2			
4D-2, 18-22(pl)		20	0.702737±12					+4.0		
4D-2, 18-22(cpx)		20	0.703901±10	0.513151± 3				+3.1		
4D-2, 18-22(wr)		20	0.702890±10		17.681± 5	15.436± 4	37.288±11			
10D-1, 21-25(wr)		36	0.702885±11		17.619±37	15.442±35	37.288±85			
13R-1, 49-56(pl)	II	45	0.702796± 8					+5.0		
13R-1, 49-56(cpx)		45	0.702909±16	0.513155± 3				+5.8		
13R-1, 49-56(amp)		45	0.702894± 5	0.513165± 3	17.494±25	15.307±21	36.899±51	+4.6	1.40	-54
13R-1, 49-56(wr)		45	0.702780±11	0.513161± 1	17.477±15	15.341±13	37.001±31			
14R-3, 127-130(amp)		55		0.513152± 7	17.524±23	15.399±20	37.193±49	+3.9	1.87	-49
15R-1, 68-72(pl)		57	0.702769±10	0.513152±28	17.513± 3	15.425± 3	37.255± 7	+4.7		
15R-1, 68-72(amp)		57	0.703412± 7	0.513137± 5				+4.4	2.20	-49
15R-1, 68-72(wr)		57	0.702848± 9	0.513164± 2	17.870± 7	15.489± 6	37.496±14			
16R-1, 0-8(amp)		62						+1.0	2.05	-51
22R-1, 56-62(amp)		95	0.702872±22	0.513195± 6				+3.4	2.02	-50
22R-1, 56-62 (vein pl)		95	0.702856±13	0.513123± 7				+4.2		
22R-1, 56-62 (host pl)		95	0.702781±16	0.513124±11	17.771±27	15.480±23	37.370±53			
23R-2, 43-47(amp)		102	0.702805±11	0.513138± 2	17.830± 7	15.515± 6	37.643±14		1.67	-54
23R-4, 122-128 (bas)		105	0.702733±16							
23R-4, 122-128 (bas) r		105	0.702756±11	0.513145± 4						
26R-2, 48-55(GR amp)		118	0.702874±10	0.513143± 3	17.875±54	15.623±47	37.851±115	+3.8	2.18	-50
26R-2, 48-55(BR amp)		118	0.702863±10	0.513155± 4	17.870±29	15.691±26	38.001±62	+4.6	1.87	-53
30R-3, 137-139(pl)		141	0.702819± 9	0.513134±13	17.524± 4	15.404± 3	37.204± 9			
30R-3, 137-139(cpx)		141	0.703251±12	0.513151± 3						
30R-3, 137-139(wr)		141	0.702902±11	0.513132± 6	17.598± 2	15.428± 2	37.288± 5			
32R-1, 55-61(pl)		149	0.702839±10					+4.0		
32R-1, 55-61(cpx)		149	0.702989±10	0.513126± 1				+3.3		
32R-1, 55-61(wr)		149	0.702926±26	0.513111± 1	17.561± 3	15.423± 3	37.228± 6			
34R-4, 3-4 (pl)		163	0.702847±18					+3.9		
34R-4, 3-4(pl) r		163	0.702869± 6		17.629±22	15.324±19	36.951±46			
34R-4, 3-4 (cpx)		163	0.703427±22	0.513186± 7				+5.1		
34R-4, 3-4(wr)		163	0.702839±11							

two pyroxenes, and the low-calcium pyroxene may be either primary orthopyroxene or inverted pigeonite. Also recovered from this interval were several leucocratic veins, the largest of which was analyzed and found to have a trondhjemitic composition. The rocks from this interval are the most evolved in the recovered core and have the lowest Mg numbers and normative An contents. These rocks are also unusual in their extreme enrichment in TiO_2 and niobium (Fig. 5). The upper contact of this unit with Unit III is marked by a 60-cm-thick mylonitic zone. The lower contact with Unit V consists of a 2- to 3-m-thick layer of mylonitized oxide-rich gabbro, which has a sharp lower contact with a brecciated olivine gabbro at the top of Unit V.

Below Unit IV, the overall degree of alteration and deformation decreases and Unit V begins a section of nearly pristine gabbro and olivine gabbro in which troctolites appear commonly for the first time. In general, there is a distinct lack of deformation and lack of FeTi oxide-rich zones. The troctolites have the highest concentrations of the compatible trace elements, chromium and nickel (Fig. 6), and Mg numbers range from 85 to 87. The magmas in equilibrium with these rocks would have had Mg numbers between 67 and 69, i.e., they were potentially in equilibrium with mantle peridotite.

Similar to Unit V, Unit VI is an olivine-rich gabbro having frequent layers of troctolites, but differs from the above sequence by being slightly more olivine-rich on average and

Table 1 (continued).

Core, Section, Interval (cm)	Lithologic Unit	Depth	$^{87}Sr/^{86}Sr$	$^{143}Nd/^{144}Nd$	$^{206}Pb/^{204}Pb$	$^{207}Pb/^{204}Pb$	$^{208}Pb/^{204}Pb$	$\delta^{18}O$	H_2O (wt%)	δD
38R-4, 112-120 pl	III	188	0.702740±16							
38R-4, 112-120 cpx		188	0.702846±19	0.513175± 7						
38R-4, 112-120 wr		188	0.702739±14	0.513129± 3	17.669±18	15.488±16	37.384±39			
41R-4, 30-38(pl)		201			17.451± 7	15.450± 6	37.294±14	+5.2		
41R-4, 30-38(cpx)		201	0.702842±13	0.513178± 4	17.504±14	15.462±12	37.297±30	+4.7		
41R-4, 30-38(wr)		201	0.702779±10		17.410± 8	15.398± 7	37.129±17			
51R-3, 76-84(pl)	IV	246	0.702880±13							
51R-3, 76-84(cpx)		246	0.702801± 7		17.411± 2	15.403± 1	37.148± 3			
51R-3, 76-84(wr)			0.702805±11							
53R-5, 40-43 (Lwr)		259	0.702826±16	0.513176±10	17.422± 1	15.416± 1	37.212± 2	+7.6	1.10	-67
53R-5, 40-43 (ULwr)		259	0.702892±17	0.513175±10	17.444± 1	15.412± 1	37.217± 2			
54R-1, 115-121(pl)		259	0.702807±10		17.420± 1	15.384± 1	37.118± 3	+7.0		
54R-1, 115-121(cpx)		259	0.702982±15	0.513116± 2				+5.7		
54R-1, 115-121(wr)		259	0.702819±12	0.513175± 6	17.413± 7	15.357± 6	37.045±15			
54R-2, 37-45(wr)		265	0.702913± 9	0.513183± 7	17.416± 1	15.396± 1	37.167± 2	+7.1	0.43	-77
56R-3, 85-91(wr)		274	0.703106± 2		17.441± 4	15.406± 4	37.176± 9			
58R-3, 130-139(pl)	V	285	0.702814±11	0.513155±12	17.437± 5	15.435± 4	37.229±11			
58R-3, 130-139(cpx)		285			17.389±11	15.400±10	37.073±23			
58R-3, 130-139(wr)		285	0.702757±37	0.513166± 7						
62R-1, 80-89(pl)		301	0.702787±10	0.513168±13				+6.0		
62R-1, 80-89(cpx)		301	0.702811±11	0.513166± 4				+6.0		
62R-1, 80-89(wr)		301	0.702885±14	0.513137± 3						
63R-1, 113-120(wr)		308	0.703234±24	0.513159± 7	17.471± 2	15.426± 1	37.377± 3	+4.6	0.83	-46
66R-3, 124-126 (pl)		326	0.703519±12					+5.5		
66R-3, 124-126(pl) r		326	0.703544±13	0.513184± 2						
66R-3, 124-126 (cpx)		326	0.702936±12	0.513174± 7				+1.4		
66R-3, 124-126 (wr)		326		0.513182± 1					0.25	-69
69R-4, 0-9 (pl)		345	0.702844± 9	0.513140±17	17.475±11	15.448± 9	37.214±22	+5.3		
69R-4, 0-9(cpx)		345	0.702793±19	0.513189± 9				+5.6		
69R-4, 0-9 (wr)		345	0.702803±10	0.513150± 6	17.506± 2	15.427± 2	37.212± 5			
74R-7, 56-65(pl)		385	0.702802±11	0.513152±12				+4.6		
74R-7, 56-65(cpx)		385	0.702799±10	0.513172±14				+5.0		
74R-7, 56-65(wr)		385	0.702818±10		17.376± 8	15.448± 7	37.141±17			
76R-1, 83-91(pl)		395	0.702790± 9	0.513120±10	17.387±11	15.363±10	37.053±23	+6.1		
76R-1, 83-91(cpx)		395	0.702864±16	0.513148± 4				+5.2		
76R-1, 83-91(wr)		395	0.702728±10	0.513137± 3						

by having pervasive, weak-to-moderate deformation that persists throughout most of the unit. This unit also contains several intervals of gabbro that are rich in chromium relative to gabbro elsewhere in Hole 735B. These Cr-rich gabbros contain a bright green clinopyroxene that is distinct from the black augite found throughout the remainder of the stratigraphic column (Shipboard Scientific Party, 1989). The boundary between Units V and VI is gradational and may represent a continuous magmatic section like that of Units II and III.

Although massive gabbros predominate throughout the section, igneous layering defined by often subtle changes in modal mineralogy and grain size is common. The orientations of these fine-scale contacts, however, are extremely variable and range from horizontal to nearly vertical. Rhythmic layering like that described from large-scale layered intrusions (such as the Bushveld or Skaergaard) was not observed, which in turn suggests that gravity settling was not the general mechanism of crystal accumulation. Furthermore, at least two of the unit boundaries are clearly tectonic in origin and consist of zones of intense brecciation and alteration with marked changes in lithology across them. These boundaries occur between Units III and IV and between Units IV and V, and essentially bound the FeTi-oxide gabbros.

Thus, although tectonic processes have disrupted the stratigraphy, the gabbros from Hole 735B tend to become more evolved upward, as might be expected from an evolving magma chamber. Moreover, Figure 1 demonstrates that even in units where evolved compositions predominate (Units I

Table 1 (continued).

Core, Section, Interval (cm)	Lithologic Unit	Depth	^{87}Sr/^{86}Sr	^{143}Nd/^{144}Nd	^{206}Pb/^{204}Pb	^{207}Pb/^{204}Pb	^{208}Pb/^{204}Pb	δ^{18}O	H2O (wt%)	δD
79-6, 81-84(pl)	VI	422	0.702847±18	0.513131±13				+6.4		
79-6, 81-84(pl) r		422		0.513120± 7	17.459± 5	15.444± 5	37.243±11			
79-6, 81-84(cpx)		422	0.702803±25					+5.7		
79-6, 81-84 (cpx) r		422	0.702828±12	0.513145± 5						
79-6, 81-84(wr)		422	0.702915±10	0.513086±11	17.532±22	15.432±19	37.173±47			
79-6, 81-84(wr) r		422	0.702917± 9		17.563± 8	15.500± 7	37.390±17			
79-7, 66-75(pl)		424	0.702787±10					+6.3		
79-7, 66-75(cpx)		424						+5.0		
79-7, 66-75(wr)		424	0.702830±10	0.513113±23	17.428± 5	15.397± 4	37.162±11			
84-5, 58-68(pl)		468	0.702752±10	0.513126± 9				+5.3		
84-5, 58-68(cpx)		468		0.513160± 4	17.401± 8	15.379± 7	37.092±16	+5.0		
84-5, 58-68(wr)		468	0.702736±10							
85-6, 36-40(pl)		479	0.702997±10	0.513011±27	17.513±19	15.387±17	37.116±41	+4.4		
85-6, 36-40(pl) r		479	0.703027± 7							
85-6, 36-40(cpx)		479	0.703200±25	0.513006± 3	17.538±26	15.318±23	36.949±54	+5.6		
85-6, 36-40(wr)		479	0.702970±10		17.549±10	15.453± 9	37.271±21			
85-6, 36-40(wr) r		479	0.703028±10		17.530± 7	15.458± 7	37.294±16			
87R-5, 97-104(pl)		498	0.702759±10		17.445± 7	15.417± 6	37.196±14			
87R-5, 97-104(cpx)		498	0.702863±10	0.513146± 2						
87R-5, 97-104(wr)		498		0.513072± 6	17.448± 5	15.422± 4	37.221±10			

Note: pl - plagioclase, cpx - clinopyroxene, wr - whole rock, bas - basalt dike, L - leached, UL - unleached, r - repeat analysis. Pb concentrations determined for the following samples : 118-735B-79R-6, 81-84 (pl) - 55.8 ng; 118-735B-22R-1, 56-62 (pl) - 85.7 ng; 118-735B-69R-4, 0-9 (pl) - 184.8 ng; 118-735B-69R-4, 0-9 (cpx) - 58.9 ng.

through IV), there is a continuum of samples having Mg numbers between 80 and 82, suggesting that there was a relatively regular influx of primitive magma into the chamber.

RADIOGENEIC ISOTOPE RESULTS

Sr-, Nd- and Pb-isotope results are summarized in Table 1 and Figures 7 and 8. Shown for reference are the fields for MORBs from the Atlantic, Pacific, and Indian oceans. Disregarding those samples having obviously high ^{87}Sr/^{86}Sr values, the gabbros from Hole 735B have Sr-isotope values similar to basalts from the Indian Ocean; their Nd-isotope ratios range from values overlapping the Indian Ocean field to higher values more like those in basalts from the Atlantic Ocean. Fewer Pb-isotope data are available, but current results show a wide range of values, in comparison with the relatively narrow range of Sr- and Nd-isotope results for these same samples. Pb-isotope ratios fall within the range of Indian Ocean MORBs (Fig. 8), but range to lower ^{206}Pb/^{204}Pb values than SWIR basalts. In a plot of ^{208}Pb/^{204}Pb values vs. ^{206}Pb/^{204}Pb values, they overlap the trend for basalts from the SWIR, but extend to both lower ^{206}Pb/^{204}Pb and ^{208}Pb/^{204}Pb values. Most surprising is the wide range in ^{207}Pb/^{204}Pb (15.3–15.6) values relative to MORBs. Given the uniformity of the Sr- and Nd-isotopic ratios for these samples, this variation is larger than one expects for primary mantle-derived magmas. The data are shown in an expanded view in Figure 9. All data in this diagram have 1σ errors <0.01 and did not show significant fractionation of isotopes during the analytical run. However, most plagioclase separates fall on a trend parallel to the ^{207}Pb/^{206}Pb fractionation line defined by the NBS 981 standard. This suggests that much of the variation in ^{207}Pb/^{204}Pb values is a fractionation effect and a function of the analytical difficulties encountered when analyzing samples having low Pb levels (50–200 ng), such as the Leg 118 gabbros (see footnote to Table 1). Nonetheless, there is a significant variation in ^{206}Pb/^{204}Pb values that is unrelated to isotopic fractionation during analysis and that we think is a real variation within the core samples recovered. Therefore, we will restrict our discussion of Pb-isotope variations to ^{206}Pb/^{204}Pb ratios.

The Sr-, Nd- and Pb-isotope results for Leg 118 gabbros define a unique field relative to other oceanic samples (Fig. 10) The ^{206}Pb/^{204}Pb ratios of Hole 735B gabbros are among the lowest recovered from the ocean basins and are lower than all those from the SWIR except the unusual sample, D5, analyzed by Hamelin and Allégre (1985). In addition, some of these gabbros are unlike any of the Indian Ocean MORBs analyzed to date in having high ^{143}Nd/^{144}Nd values, more like MORBs from the Atlantic or Pacific oceans, while ^{87}Sr/^{86}Sr values are similar to other Indian Ocean MORBs. Thus, the mantle source for the gabbro parental magma may have had lower time-integrated U/Pb and higher Sm/Nd ratios than most Indian Ocean MORBs, but similar Rb/Sr ratios.

Figure 11A presents a summary of the Sr-isotope variations with depth i-n both whole-rock and separated mineral samples. This figure demonstrates that the Leg 118 gabbros exhibit significant variations in isotopic composition, but that most of that variation occurs in the clinopyroxene. Analyses of gabbro whole-rock and plagioclase separates (with one exception) show a relatively small range of ^{87}Sr/^{86}Sr values of 0.7027 to 0.7030 (plagioclase from hydrothermal vein sample, 118-735B-66R-3, 124-126 cm, has a Sr-isotope value of 0.7035). In contrast, clinopyroxene exhibits a much wider range of ^{87}Sr/^{86}Sr values of 0.7028 to 0.7039. Most samples are

Table 2. Petrographic summary of Leg 118 gabbros.

Core, Section, Interval (cm)	Lithologic Unit	Rock name	Plag	Cpx	Opx	Ol	Oxides	Amph	Others	Alteration	Grain size	Texture
1D-2, 80-83		Metagabbro norite	X	X	X		M	Br>Gr	Clay	V. ext.	Fine to coarse	Porphyroclastic
4D-2, 18-22	I	Metagabbro norite	X	X	R		M	Gr>Br	Clay, tremolite	V. ext.	Fine to med.	Porphyroclastic
10D-1, 21-25		Metagabbro	X	X		R	M	Gr>Br	Clay	Ext.	Fine to coarse	Porphyroclastic
13R-1, 49-56		Metagabbro	X	X		R	M	Gr+Br	Sphene,talc zircon,tremolite	Ext.	Fine to coarse	Mylonitic/ porphyroclastic
14R-3, 127-136		Metagabbro	X	X				Gr+Br		Mod.	Coarse	Granular
15R-1, 68-72		Amphibolitized metagabbro	X					Gr		V. ext.	Coarse	Porphyroclastic
16R-1, 0-8		Metagabbro	X	X		R	M	Gr	Talc	V. ext.	Fine to coarse	Porphyroclastic
22R-1, 56-62		Foliated gabbro w/ amph + plag vein	X	X				Br>Gr		Mod. to v. ext.	Med.	Granular
23R-2, 43-47		Ilmenite microgabbro	X	R			M+I	Br		V. ext.	Med.	Granular
23R-4, 122-128		Aphyric basaltic dike	X	X		X	M	Gr	Clay	Min.	Fine	Intersertal
26R-2, 48-55 (Br)		Amphibolitized metagabbro/	X	R			M+I	Br		V. ext.	Med.	Porphyroclastic
26R-2, 48-55 (Gr)		Metagabbro contact	X	R			M	Gr		Ext.	Coarse	Granular
30R-3, 137-139		Amphibolitized ilm. gabbro	X	X			M+I	Br+Gr		Ext.	Coarse	Granular to porphyroclastic
32R-1, 55-61		Ilmenite gabbro	X	X			M+I	Br+Gr	Sphene, clay, chlorite	Minor	V. coarse	Mesocumulate
34R-4, 3-4		Ilmenite gabbro	X	X	Ex		M+I	Br+Gr	Apatite	Minor	V. coarse	Mesocumulate
38R-4, 112-120		Olivine gabbro w/ carbonate vein	X	X				Gr+Br	Carb., clay, oxidation by vein	Minor	Coarse	Granular
41R-4, 30-38	III	Olivine gabbro	X	X		X	M	Br+Gr	Talc	V. minor	Med. to coarse	Granular

Note: X denotes mineral phase present; R - presence of mineral phase interpreted from replacement phase mineralogy and texture; Ex - exsolution of opx from cpx; G - high Cr green cpx; M - magnetite; I - ilmenite; Br - brown amphibole; Gr - green amphibole (relative proportions of brown to green amphibole denoted as greater than (>), less than (<) and subequal (+). Extent of alteration given in relative terms: v. minor - <5%; minor - 5%-25%, moderate - 25%-50%, extensive - 50%-75%, and v. extensive - 75%-100%.

less than 0.7030, however, similar to the plagioclase and whole-rock values. In samples where coexisting plagioclase and clinopyroxene were measured, clinopyroxene is typically higher than plagioclase. Similarly, Nd- and Pb-isotope values for most separated plagioclase are lower than those from whole rock samples or coexisting clinopyroxene (Figs. 11B and 11C). Some of these systematic mineral variations may reflect the fractionation of Sm/Nd and Rb/Sr during crystallization 12 Ma ago, but taken collectively, the range of isotopic compositions encountered suggests that either a range of isotopically distinct parental magmas entered the magma chamber beneath this portion of the SWIR and/or late-stage alteration has selectively affected different portions of the gabbroic section.

Such results indicate that the mineral and whole-rock isotopic variations are exceedingly complex. Nd-isotope ratios show little systematic variation with depth (Fig. 11B), except toward the bottom of the hole where the Cr-rich gabbros occur. By contrast, Pb-isotope ratios exhibit a strong enrichment in $^{206}Pb/^{204}Pb$ in the top 200 m of Hole 735B, similar to Sr-isotopes values. Thus, the degree of mineral disequilibrium and the amount of whole-rock variation in Sr- and Pb-isotopes is more pronounced at higher levels—as are the effects of alteration and deformation. Many of the high $^{87}Sr/^{86}Sr$ ratios are found in clinopyroxene and probably reflect a locally extensive replacement by amphibole, while coexisting plagioclase is simply recrystallized. More importantly, high $^{87}Sr/^{86}Sr$ and $^{206}Pb/^{204}Pb$ values occur generally where introduction of seawater was facilitated by late-stage fracture porosity, as in the brecciated zone between Units IV and or at the exposed top of the section. Considerable fracture permeability was indicated for these upper units by high measured flow rates during drill-stem packer tests (Goldberg and Becker, 1988), when compared with that of the relatively impermeable lower units. It is interesting, however, that secondary amphiboles do not have consistently high Sr-isotope values; of those samples analyzed, only one has an $^{87}Sr/^{86}Sr$ ratio greater than 0.703. More than one generation of

Table 2 (continued).

Core, Section, Interval (cm)	Lithologic Unit	Rock name	Plag	Cpx	Opx	Ol	Oxides	Amph	Others	Alteration	Grain size	Texture
51R-3, 76-84	IV	Ilmenite gabbro	X	X			M+I	Gr+Br		Mod.	V. coarse	Granular
53R-5, 40-43		Trondhjemite	X	X			M		Qtz, biotite	V. minor	Med.	Granular
54R-1, 115-121		Olivine ilmenite metagabbro	X	X		X	M+I	Br+Gr	Mica, apatite	Ext.	Med.	Porphyroclastic
54R-2, 37-45		Felsic hydrothermal vein	X	X					Biotite		Med.	Plag + cpx symplectites
56R-3, 85-91		Amphibolitized gabbro	X	X			M	Br+Gr	Chlorite, sphene zoisite	Ext.	Coarse	Granular
58R-3, 130-139	V	Olivine gabbro	X	X		X	M	Gr	clay	V. minor	Coarse	Mesocumulate
62R-1, 80-89		Olivine gabbro	X	X		X	M		Clay	V. minor	Coarse	Mesocumulate
63R-1, 113-120		Hydrothermal felsic vein	X	X					Clinozoisite,clay sphene, chlorite	V. ext.	Med.	Granular
66R-3, 124-126		Hydrothermal felsic vein	X	X					Clay	V. ext.	Fine to coarse	Granular
69R-4, 0-9		Olivine gabbro	X	X		X	M	Br	Clay	V. minor	Coarse	Mesocumulate
74R-7, 56-65		Olivine gabbro	X	G		X	M	Br	Clay	V. minor	Coarse	Mesocumulate
76-1,83-91cpx		Ilmenite gabbro	X	X			M+I	Gr>Br		Minor	V. coarse	Mesocumulate
79R-6, 81-84	VI	Olivine gabbro	X	G		X	tr	Br	Clay	V. minor	Coarse	Mesocumulate
79R-7, 66-75		Olivine gabbro	X	X		X	M	Br	Clay	V. minor	Coarse	Mesocumulate
84R-5, 58-68		Olivine gabbro	X	X		X	tr	Br	Clay	V. minor	Coarse	Mesocumulate
85R-6, 36-40		Olivine gabbro	X	G		X	tr	Br	Clay	V. minor	Coarse	Mesocumulate
87R-5, 97-104		Olivine gabbro	X	X		X	M	Br+Gr	Clay, talc	Minor	Med. to coarse	Porphyroclastic

Note: X denotes mineral phase present; R - presence of mineral phase interpreted from replacement phase mineralogy and texture; Ex - exsolution of opx from cpx; G - high Cr green cpx; M - magnetite; I - ilmenite; Br - brown amphibole; Gr - green amphibole (relative proportions of brown to green amphibole denoted as greater than (>), less than (<) and subequal (+). Extent of alteration given in relative terms: v. minor - <5%; minor - 5%-25%, moderate - 25%-50%, extensive - 50%-75%, and v. extensive - 75%-100%.

secondary amphibole can be identified petrographically in Leg 118 gabbros—a high-temperature hornblende, generally associated with areas of plastic deformation, and a lower-temperature actinolitic amphibole seen more commonly in areas of static alteration replacing primary phases and in late-stage veins. However, amphiboles of each type were analyzed and no systematic difference was apparent. Still, the one amphibole sample that does have significantly elevated Sr-isotope ratios is from a gabbro that had been extensively amphibolitized by actinolitic amphibole.

Samples from the lower portion of the stratigraphic column exhibit trends toward higher $^{87}Sr/^{86}Sr$, higher $^{206}Pb/^{204}Pb$, and lower $^{143}Nd/^{144}Nd$ values. Because samples from the lower 250 m exhibit little visible evidence for secondary alteration (see Table 2), this range in isotopic values is thought to be a primary feature that is related to the introduction of isotopically distinct magma batches into the magma chamber. The compositions of these samples will be discussed below in terms of stable isotopes.

OXYGEN AND HYDROGEN ISOTOPE RESULTS

The oxygen and hydrogen isotope results are listed in Table 1 and are shown graphically in Figures 12 through 14. In contrast to the relative uniformity in radiogenic isotope values over much of the gabbro column, O-isotope ratios vary significantly throughout and deviate markedly from average unaltered MORB ($\delta^{18}O \approx +5.7$‰). Gabbro pyroxene and plagioclase separates show wide ranges and extend to relatively low values of $\delta^{18}O$, +1.4 to +6.0‰, and +3.9 to +7.0‰, respectively. When plotted as a function of depth, the lowest values can be seen in the upper part of the section and the highest value, +7.6‰, occurs in the quartz-bearing trondhjemite. Altered rocks adjacent to the trondhjemite also have elevated $\delta^{18}O$ values. In a plot of $\delta^{18}O_{cpx}$ vs. $\delta^{18}O_{plag}$ (Fig. 13), the data exhibit a distribution similar to gabbroic samples from the central Indian Ridge (Stakes et al., 1984), but reach neither the low $\delta^{18}O$ values found in hydrothermally altered gabbros from subaerial environments, nor the high ratios found in the Oman ophiolite. Metagabbros from the Sarmiento ophiolite may be more similar to the Hole 735B gabbros in that whole-rock $\delta^{18}O$ values as low as +2.6‰ were observed (Elthon et al., 1984), but mineral data are not reported.

Gregory and Taylor (1986) and Gregory and Criss (1986) showed that for mineral assemblages having different bulk ^{18}O compositions equilibrated under closed-system conditions, coexsting minerals should exhibit small ^{18}O fractionations with small $\Delta_{x-y} \equiv \delta^{18}O_x — \delta^{18}O_y$ values that form tight clusters

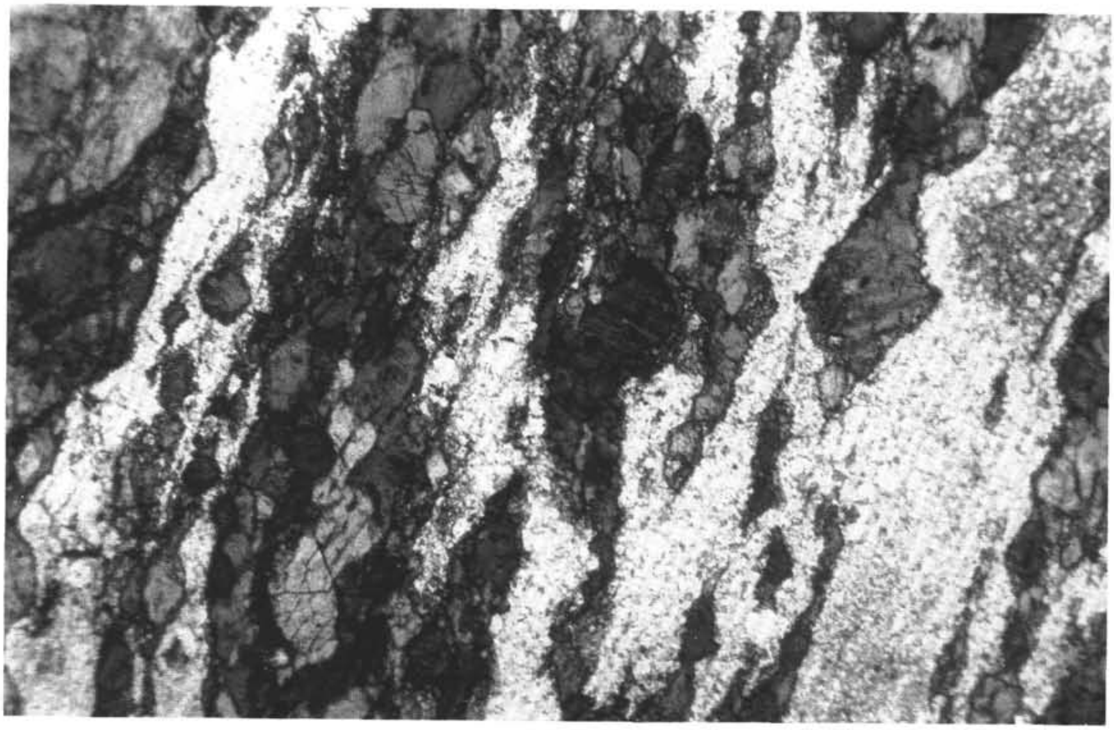

Figure 2. Photomicrograph of porphyroclastic gabbro showing a strong foliation defined by stretching of plagioclase and clinopyroxene. Plagioclase is highly recrystallized into neoblasts (Sample 118-735B-1D-2, 80–83 cm) (field of view = 3.5 mm).

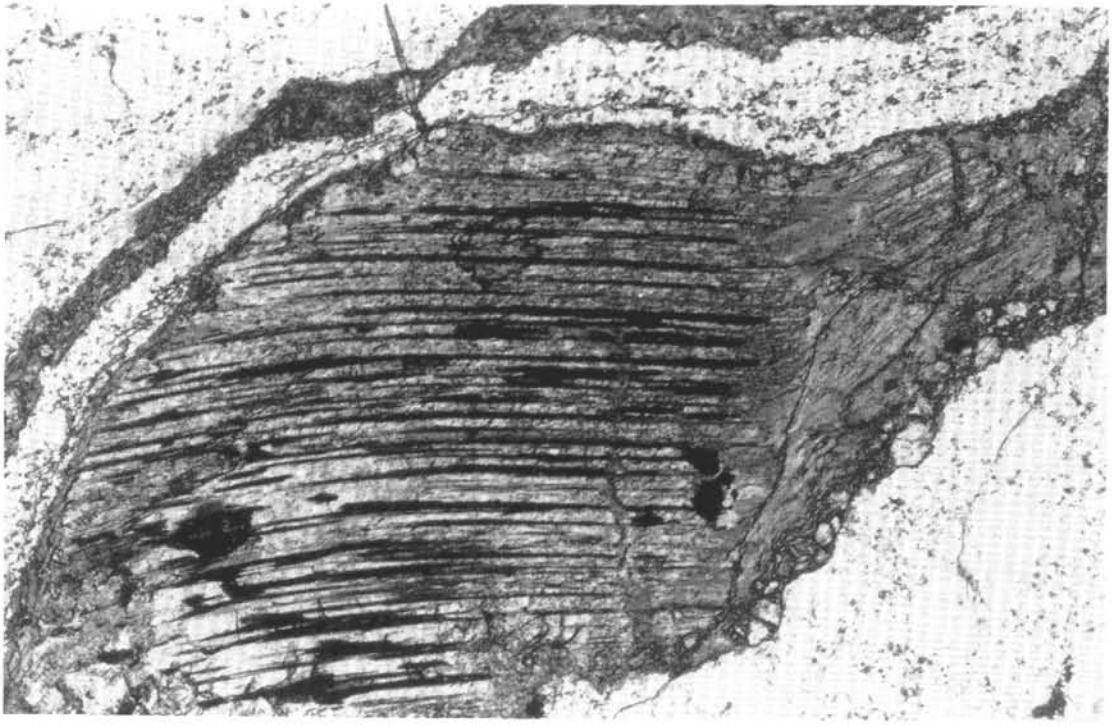

Figure 3. Photomicrograph of porphyroclastic gabbro showing stretching of clinopyroxene and extensive replacement by secondary amphibole plus magnetite (Sample 118-735B-1D-2, 80–83 cm). Field of view = 3.5 mm.

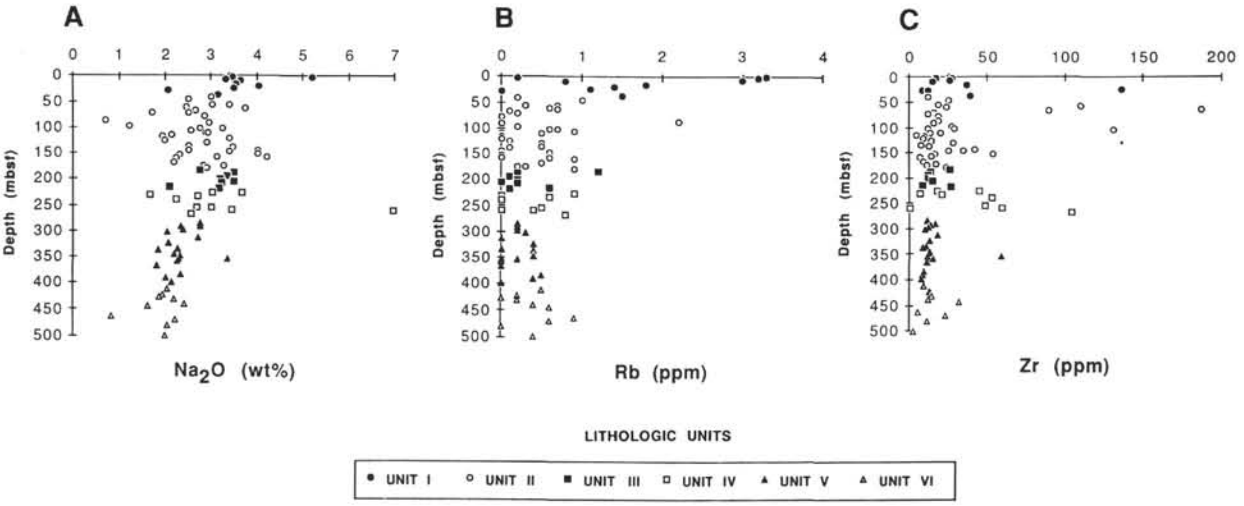

Figure 4. Variations in Na$_2$O, Rb, and Zr as a function of depth showing that magmaphile elements are generally lowest at the bottom of the section, but increase and exhibit their maximum concentrations in the uppermost units of Hole 735B. Concentrations determined by shipboard XRF.

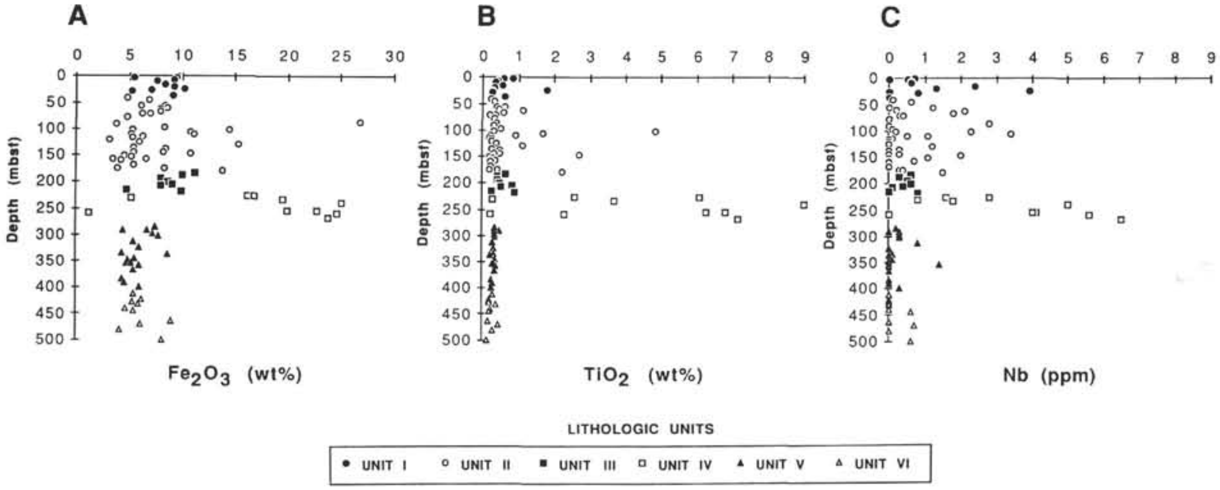

Figure 5. Variations in Fe$_2$O$_3$, TiO$_2$, and Nb vs. depth showing extreme enrichments in the middle section of Hole 735B, where FeTi oxide gabbros predominate.

or define linear arrays of 45° slope that parallel the $\Delta = 0$ fractionation line on a diagram of $\delta^{18}O_x$ vs. $\delta^{18}O_y$. At infinite temperature, Δ approaches zero, but with decreasing temperature, the array is displaced away from the $\Delta = 0$ line, with a magnitude and direction related to the equilibrium fractionation factor for the phases considered. For example, plagioclase-clinopyroxene pairs analyzed from rapidly quenched basaltic magmas have $\delta^{18}O_{plag\text{-}cpx} \approx 0.5‰$. If we accept a $\delta^{18}O$ value for average MORB of +5.7‰, the corresponding primary magmatic $\delta^{18}O_{plag}$ should be about +6.0‰ and $\delta^{18}O_{cpx}$ should be about +5.5‰ (Fig. 14). Slowly cooled plutonic gabbros typically exhibit $\delta^{18}O_{plag\text{-}cpx}$ values of +0.8 to +1.3‰ (Taylor, 1968). Thus, for closed-system equilibration to a different thermal regime, the trajectory of plagioclase-clinopyroxene pairs in $\delta^{18}O$ vs. $\delta^{18}O$) will have negative slopes and fall within a right triangle similar to that shown in Figure 14. By contrast, open-system exchange with a new fluid composition results in curved mixing arrays that cut across the $\Delta = 0$ fractionation line with steep positive slopes. A detailed discussion of O-isotope open- vs. closed-system systematics is presented in Gregory and Taylor (1986) and Gregory and Criss (1986); the reader is referred to these studies for a more in-depth analysis.

For the Hole 735B gabbros, we observe a steep, curved mixing array that falls well outside the region of equilibrium, closed-system exchange in a trend characteristic of hydrothermally exchanged minerals. As such, the present $\delta^{18}O$ composition of an individual mineral is a function of several parameters. One parameter is the isotopic composition of the fluid phase; for our purposes, this is either seawater in which $\delta^{18}O \approx 0$, or a modified seawater-hydrothermal solution in which $\delta^{18}O$ equals some modified value either lower or higher than magmatic fluids. In the basalt-seawater system, temperatures of alteration in the vicinity of 250° to 300°C produce Δrock-water equal to approximately +5.7‰. Hydrothermal alteration at higher temperatures (greater than 400°C) leads to lower Δ values and, thus, depletion of the rock in ^{18}O. Also important are the water/rock ratio and the degree of isotopic

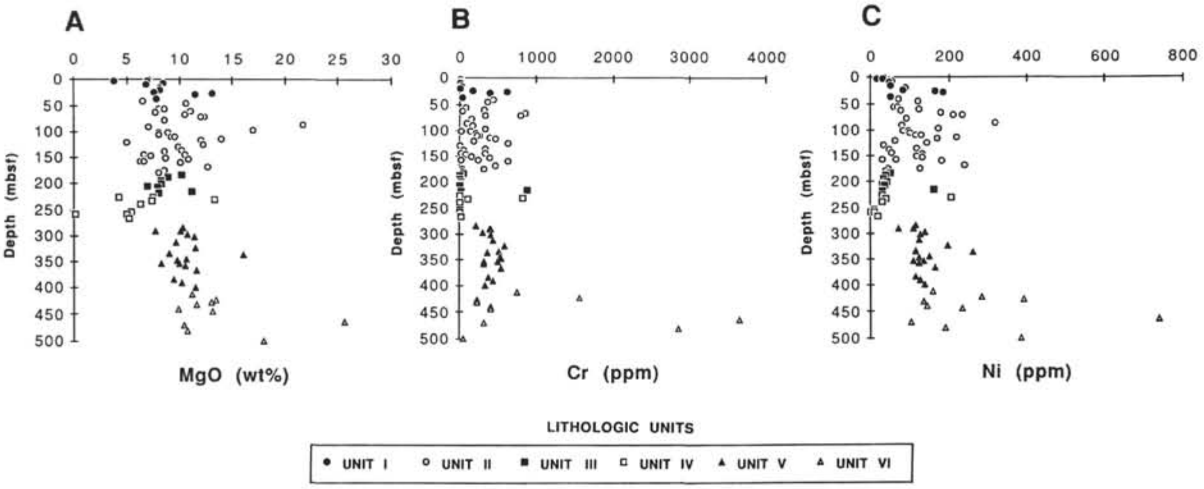

Figure 6. Variations in MgO, Cr, and Ni vs. depth showing that concentrations of compatible elements are highest in gabbros from the bottom of Hole 735B and decrease generally upward.

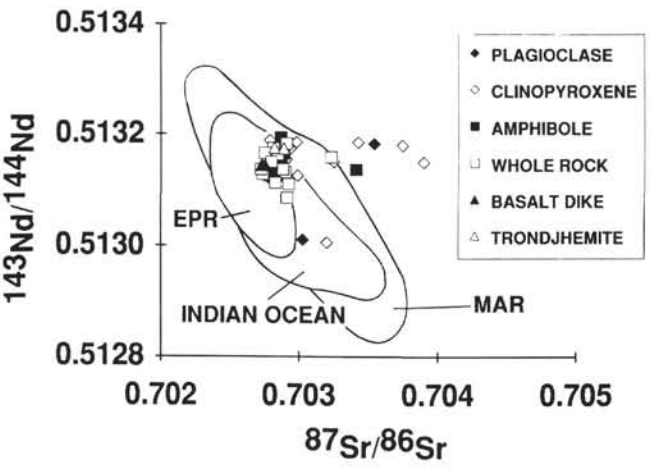

Figure 7. Plot of $^{87}Sr/^{86}Sr$ vs. $^{143}Nd/^{144}Nd$ for Leg 118 gabbros, compared with the fields for East Pacific Rise, Mid-Atlantic Ridge, and Indian Ocean basalts. EPR and MAR data from Cohen and O'Nions (1982), Ito et al. (1987), White et al. (1987), Shirey et al. (1987), Cohen et al. (1980) and Macdougall et al. (1986). Indian Ocean data from Ito et al. (1987), Cohen et al. (1980), Hamelin et al. (1985/1986), Dupré and Allégre (1983), Hamelin and Allégre (1985), Price et al. (1986), Michard et al. (1986), and Hedge et al. (1979).

equilibrium that has been attained. The nature of the Hole 735B gabbros array indicates that these gabbros experienced open-system exchange with seawater at relatively high temperatures and that for the same conditions of temperature and fluid composition, plagioclase has exchanged at a faster rate than that for coexisting clinopyroxene, i.e., the $\Delta_{plag\ cpx}$ is reversed (Fig. 14). In the most altered samples, clinopyroxene also exchanged substantially, and the ^{18}O fractionation between plagioclase and clinopyroxene reverts to a value approaching equilibrium, but at lower $\delta^{18}O$ for both plagioclase and clinopyroxene. Hydrothermal vein Sample 118-735B-66R-3, 124–126 cm, is unusual in having an extremely low $\delta^{18}O$ clinopyroxene value (+1.4‰), but relatively normal plagioclase ratios (+5.5‰). The reason for this is not understood, but may reflect isotopic overprinting of low-temperature alteration processes on the plagioclase, but not on the clinopyroxene. Nevertheless, assuming a hydrothermal fluid composition of $\delta^{18}O = 0$ (e.g., seawater), estimates of the water/rock ratios necessary to produce most of the $\delta^{18}O$ values are still low (<1).

Similarly, the uniformly low O-isotope values for amphibole (+3.8 to +4.6‰) combined with D/H ratios of −49 to −54‰ indicate that these minerals did not crystallize from pure magmatic waters ($\delta^{18}O \approx +5.7$‰ and δD of −80‰), but from fluids having significantly lower $\delta^{18}O$ and higher δD values. Over a wide range in temperatures at equilibrium, the common hydrous minerals all have D/H ratios of about 30 to 60‰ lower than their coexisting waters. Thus, all amphiboles from the Mid-Atlantic Ridge, the central Indian Ridge and from ophiolites have δD values between −30 and −60‰ and $\delta^{16}O$ values of +2 to +6‰. The Hole 735B amphiboles also fall within this range. However, the fact that most Hole 735B amphiboles have $^{87}Sr/^{86}Sr$ values indistinguishable from the primary mineral phases suggests that the Sr-isotope composition of the hydrothermal fluids was buffered in most places by the magmatic pile, rather than by the isotopic composition of seawater.

DISCUSSION

Effects of Hydrothermal Alteration

The net effect of hydrothermal activity on the chemistry of the oceans is a matter of considerable debate (Hart and Staudigel, 1982). Large fluxes have been documented at black smokers and within some portions of the upper oceanic crust. But what happens in the lower portions of the crust? This question has particular relevance when one considers that the lower oceanic crust may constitute 50% or more of the material recycled into the mantle. Furthermore, the depth of penetration of hydrothermal activity in the crust is central to evaluating hydrothermal circulation patterns at ridges and the mechanisms of removing heat from the crust. Based on a strong constrast in grain size between gabbros and crosscutting dikes observed in ophiolites, scientists have suggested that these gabbros underwent relatively rapid cooling before emplacement of a particular dike. This has been considered evidence for hydrothermal convective (rather than conductive) cooling of the upper part of the oceanic crust as it travels away from the axial zone (Anderson et al., 1985; Lister, 1984). Models of hydrothermal circulation and the heat budget for black smokers in the ocean crust also suggest that seawater rapidly cools the upper portions of the magma chamber, but these models are

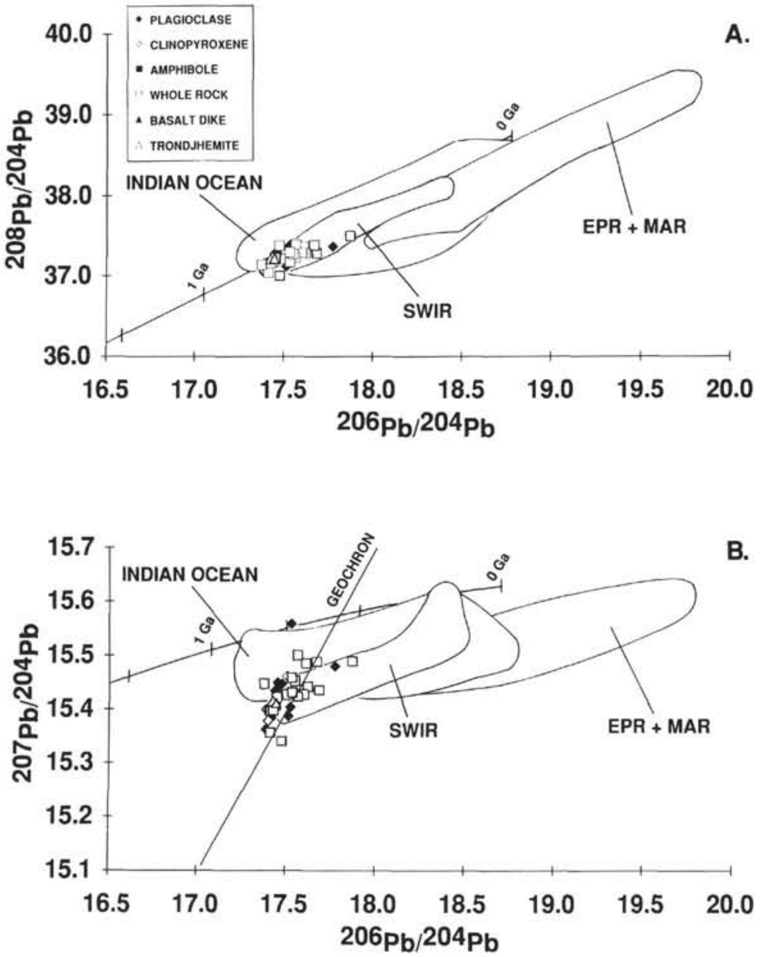

Figure 8. Plot of $^{206}Pb/^{204}Pb$ vs. $^{207}Pb/^{204}Pb$ (**B**) and $^{208}Pb/^{204}Pb$ (**A**). Data for EPR, MAR, and Indian Ocean MORBs are from the same sources as given in Figure 7.

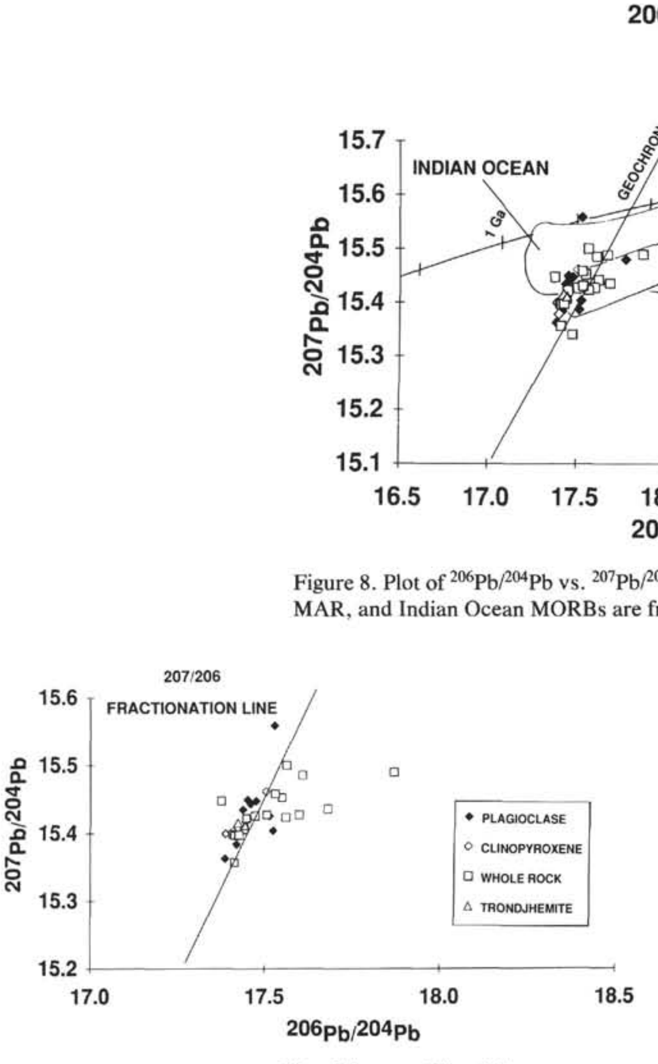

Figure 9. Expanded view of $^{206}Pb/^{204}Pb$ vs. $^{207}Pb/^{204}Pb$ for Leg 118 gabbro whole-rock samples and mineral separates relative to the $^{207}Pb/^{206}Pb$ fractionation line. All data in this diagram have 1σ errors less than 0.01. Symbols as in Figure 8.

less specific about the depth to which seawater circulates. However, on the basis of radiogenic and stable isotopic data for the Oman ophiolite, Gregory and Taylor (1981) suggested a hydrothermal system for the total ocean crust in which seawater circulates throughout the layered gabbro, cooling and ultimately altering it.

These models of hydrothermal alteration in the lower crust apparently conflict with existing radiogenic isotopic results for Leg 118 gabbros. The generally low $^{87}Sr/^{86}Sr$ values observed in these rocks suggest little interaction with seawater, even for highly altered and deformed samples. However, the $\delta^{18}O$ composition of plagioclase is known to respond quickly to hydrothermal alteration and should reflect interaction with a low ^{18}O fluid such as seawater even before other geochemical effects have been registered (Gregory and Taylor, 1981). Such an effect was noted by Stakes et al. (1984) for gabbros from the central Indian ocean. These authors pointed out that the apparent pristine petrological condition of some oceanic gabbros is misleading because the plagioclase grains in all but a few analyzed samples have undergone thorough O-isotope exchange, which lowered the $\delta^{18}O$ of the feldspar from its primary value of +6.1 to +6.4‰ to values of +5.0 to +6.0‰; the general paucity of hydrous minerals in these samples indicates that alteration occured at very high temperatures or relatively low water/rock ratios, or both. However, this study of oceanic gabbros and others from ophiolite sequences (McCulloch et al., 1981; Gregory and Taylor, 1981) equate decreasing $^{18}O/^{16}O$ ratios with increasing $^{87}Sr/^{86}Sr$ for high-temperature hydrothermal alteration. This sort of behavior is not well represented in the Hole 735B gabbros (Fig. 15). Instead, the Sr-isotope composition seems to be buffered by the magmatic pile. As shown in Figure 11A, most whole-rock samples and mineral separates exhibit only

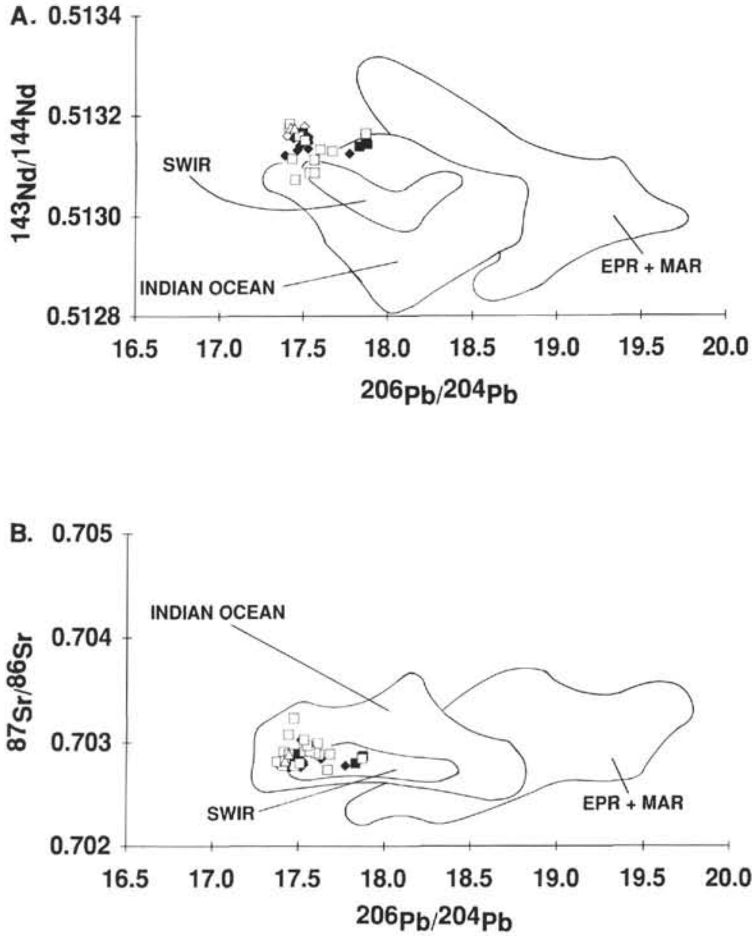

Figure 10. Plot of $^{206}Pb/^{204}Pb$ vs. $^{143}Nd/^{144}Nd$ (**A**) and $^{87}Sr/^{86}Sr$ (**B**) for Leg 118 gabbros showing their unique isotopic composition relative to MORBs from the EPR, MAR, and Indian Ocean. Symbols as in Figure 8.

a limited range in $^{87}Sr/^{86}Sr$ values, even though they describe a wide range in $\delta^{18}O$ (Figs. 11 and 15). Only in the uppermost units, where more evidence for low-temperature alteration can be seen, is there an indication of elevated $^{87}Sr/^{86}Sr$ values, and these elevated ratios are found only in clinopyroxene and/or amphibole separates, (???) connecting clinopyroxene or amphibole and coexisting plagioclase from Samples 118-735B-4D-2, 18–22 cm; 118-735B-15R-1, 68–72 cm; and 118-735B-1D-2, 80–83 cm (left to right). This is shown in Figure 16 by lines having steep negative slopes. Note that each of these samples comes from a depth of less than 60 m in Hole 735B. Two samples from deeper in Hole 735B, Samples 118-735B-66R-3, 124–126 cm, and 118-735B-34R-4, 3–4 cm, exhibit the more unusal behavior that the phase having the lowest $\delta^{18}O$ also has the lower $^{87}Sr/^{86}Sr$. For sample 118-735B-66R-3, 124-126 cm, the situation is even more complicated in that the phase with the highest $^{87}Sr/^{86}Sr$ is plagioclase rather than clinopyroxene. The isotopic compositions of these two samples are not well understood, but these data may be isotopic evidence that alteration has occurred over a range of temperatures and that in some samples, the contrasting isotopic effects of high and low temperature alteration are superimposed.

In contrast to the uniformity of whole-rock $^{87}Sr/^{86}Sr$ values throughout Hole 735B, Pb-isotopes values from the upper 200 m are significantly higher than those from the relatively unaltered samples lower in the stratigraphic column. The abundance levels of Pb and Nd in seawater are low enough that interaction with seawater should not effect Pb-isotope ratios (Hart and Staudigel, 1989). Similarly, geochemical data from high-temperature axial hot springs (Hart and Staudigel, 1989, and references therein) show that neither Sr, Th, nor the REE are strongly mobilized in the deeper crust. However, Rb appears to be strongly extracted, Pb is mildly extracted, and U is strongly added to the lower crust by high-temperature, hydrothermal alteration. Thus, altered layer 3 gabbros potentially have high U/Pb, low Th/U, and unchanged Sm/Nd values. Nonetheless, if the range in $^{206}Pb/^{204}Pb$ ratios between altered and unaltered Leg 118 gabbros is caused by isotopic evolution over the past 12 Ma, their μ values should differ by approxmately 250. Thus, it seems more likely that the $^{206}Pb/^{204}Pb$ enrichment observed is a function of alteration, similar to the effect shown by Sr-isotopes.

TRONDHJEMITE AND THE ORIGIN OF HIGH $\delta^{18}O$ VALUES IN HOLE 735B

In contrast to the ^{18}O depletion recorded in most of the Hole 735B gabbros, the trondhjemite dike has a relatively high $\delta^{18}O$ value (+7.6‰). One explanation for this is that the stabilization of quartz in the primary mineral assemblages resulted in a heavier O-isotope whole-rock composition. However, quartz constitutes only about 20% of the trondhjemite,

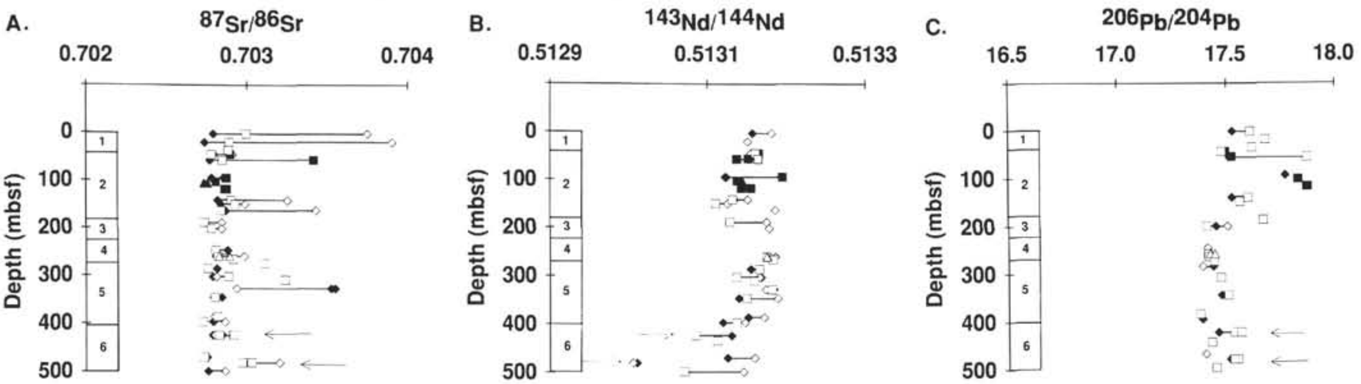

Figure 11. Radiogenic isotope composition vs. depth. A. Summary of $^{87}Sr/^{86}Sr$ variations for whole-rock samples and constituent mineral phases. Solid line connects mineral and whole-rock analyses for the same sample. Unit boundaries are shown on the left-hand side of each column. Arrows denote Cr-rich samples containing green diopside (see Table 2). B., C. Summaries of Nd- and Pb-isotopes, respectively. Symbols as in Figure 8.

and its $\delta^{18}O$ value would have to be far heavier than that predicted by equilibrium fractionation factors to produce such a high $^{18}O/^{16}O$ ratio in the whole rock. Furthermore, this mechanism cannot explain the elevated $\delta^{18}O$ of the plagioclase in adjacent intervals of gabbro, nor an H-isotope composition that is intermediate between primary magmatic water and the high D/H ratios shown by secondary amphiboles. Thin veins of plagiogranite within the high-level gabbros of the Samail ophiolite have $\delta^{18}O$ values of +7.1 to +7.7‰ (Stakes et al., 1984). These veins were interpreted as late-stage melts, filter-pressed from pegmatitic borders surrounding partially assimilated, altered roof rocks that were incorporated into the upper levels of the magma chamber by stoping. Typically, these roof rocks are enriched in ^{18}O from hydrothermal interaction with the highly modified seawater that produced ^{18}O depletions in the underlying gabbros. A similar mechanism may be resonsible for the high $\delta^{18}O$ of the Hole 735B trondhjemite. If so, this implies that the 500-m section of gabbro recovered is from the upper portions of the magma chamber.

Alternatively, the high $\delta^{18}O$ value of the trondhjemite may be the product of enrichment of ^{81}O by magmtic differentiation, similar to the model proposed by Elthon et al. (1984) for the Sarmiento ophiolite. Many of the plutonic rocks in the Sarmiento ophiolite contain greater than 25% magnetite-ilmenite crystals that formed during the final stages of crystallization of ferrobasaltic magmas. Because magnetite has a much lower $\delta^{18}O$ value than co-precipitating pyroxenes, amphiboles, feldspars, or quartz, crystallization of significant amounts of magnetite will increase the $\delta^{18}O$ of the residual magma. The thick section of magnetite+ilmenite-bearing gabbros from Hole 735B suggests that significant enrichment of ^{18}O could be produced during the final, extreme stages of magmatic differentiation. Thus, for the magma chamber represented by the Hole 735B gabbros, the trondhjemite is the culmination of differentiation processes.

HETEROGENEITY OF GABBRO PARENTAL MAGMA COMPOSITIONS

Most gabbros from Units V and VI exhibit little visible evidence for alteration; petrographically, they are free of secondary alteration minerals (see Table 2). Furthermore, the

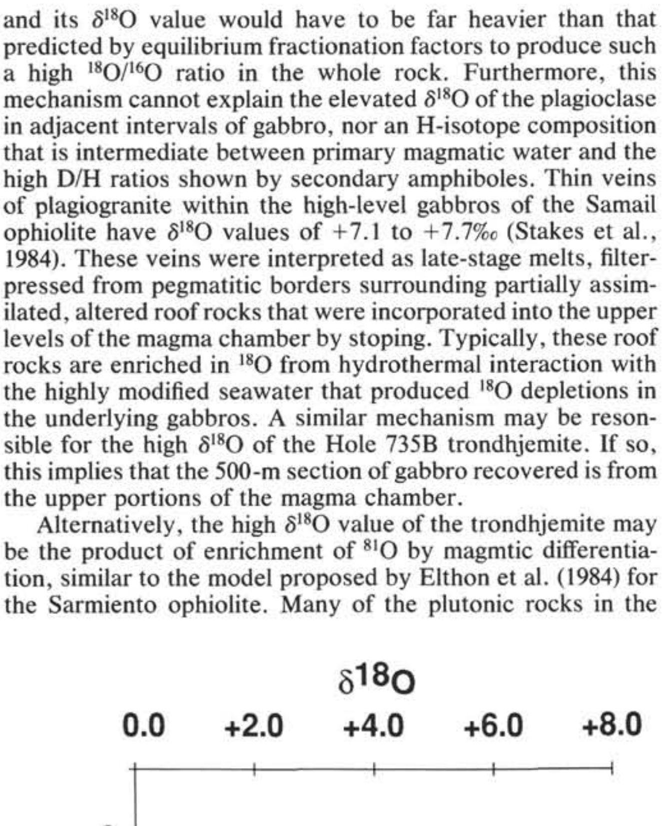

Figure 12. Plot of O-isotope composition vs. depth for Hole 735B gabbros. Symbols as in Figure 8.

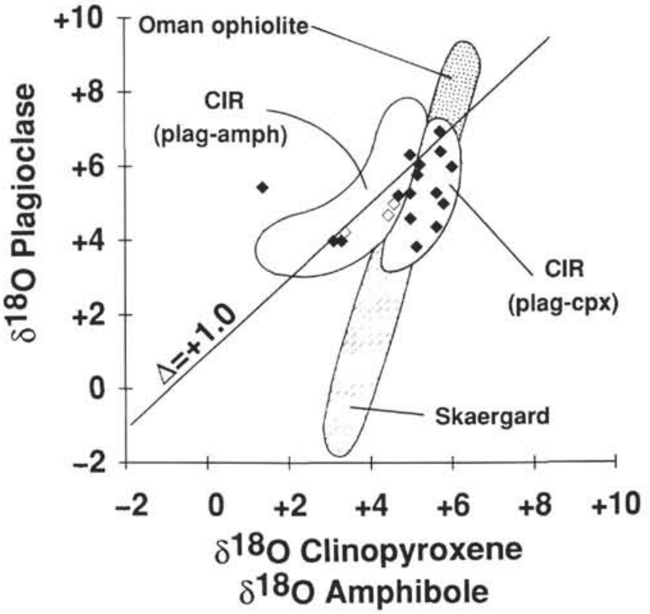

Figure 13. Plot of $\delta^{18}O_{cpx}$ vs. $\delta^{18}O_{plag}$ showing disequilibrium relationship between the mineral phases. Field for Oman gabbros from Gregory and Taylor (1981). Solid circles indicate plagioclase-clinopyroxene pairs; open circles represent plagioclase-amphibole pairs.

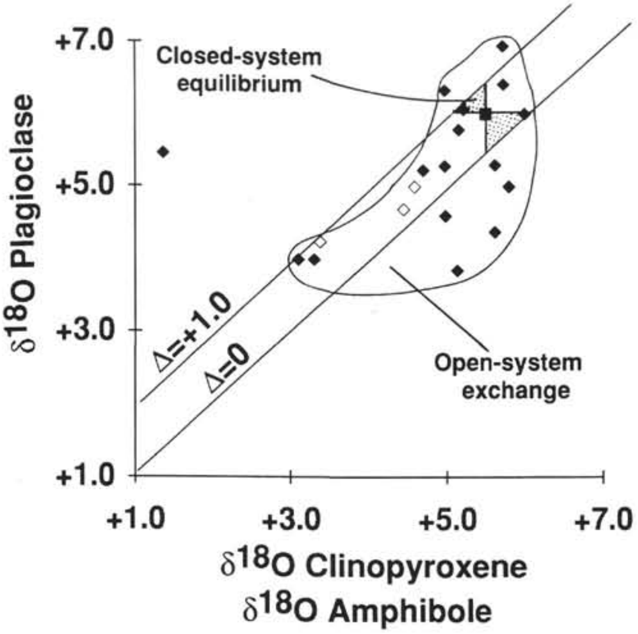

Figure 14. Plot of $\delta^{18}O$ plagioclase vs. $\delta^{18}O$ clinopyroxene for samples of cumulate gabbro from Hole 735B. These data plot outside the fields of closed-system equilibrium cooling.

differences in $^{87}Sr/^{86}Sr$ ratios between minerals and whole rock samples are small (see Fig. 11). However, the measured $^{87}Sr/^{86}Sr$ ratios in both whole rock and separated phases are high (0.7028–0.7030), and O-isotope disequilibrium is observed between coexisting plagioclase and clinopyroxene because of relatively low $^{18}O/^{16}O$ ratios in the plagioclase. As discussed in the previous section, these O-isotope characteristics are indicative of open-system hydrothermal exchange with seawater. This might lead one to assume that the elevated $^{87}Sr/^{86}Sr$ values for some of the samples from the lower units result from the same process, but several observations suggest that this is not the case. First, the clinopyroxene $\delta^{18}O$ values from these units are high (+5.0 to +6.0‰) and apparently unaffected by the hydrothermal fluids that have depleted the coexisting plagioclases in ^{18}O. If the Sr-isotopes are affected by interaction with seawater at high temperatures and the plagioclase records high-temperature hydrothermal exchange with a low-^{18}O fluid, it is difficult to envisage how the $^{18}O/^{16}O$ ratio could be left unchanged. Furthermore, the increase in $^{87}Sr/^{86}Sr$ values toward the base of the section is accompanied by lower $^{143}Nd/^{144}Nd$ values (Fig. 12b) and higher $^{206}Pb/^{204}Pb$ values (Fig. 11C), particularly in Sample 118-735B-85R-6 36–40 cm. Because Nd-isotopes are not readily affected by hydrothermal alteration, it seems unlikely that the Sr- and Pb-isotopic compositions of these samples result from this process. Therefore, we prefer to interpret the Sr-isotopic composition of these rocks as a primary feature indicative of their parental magma composition.

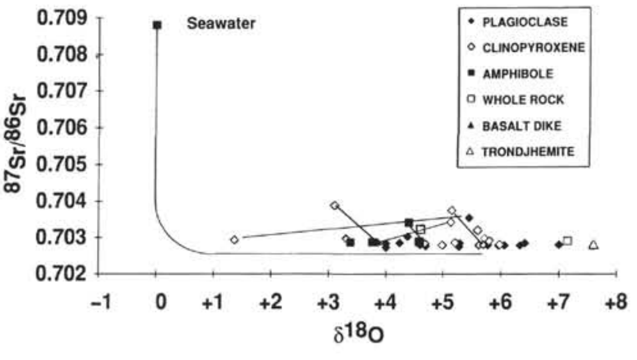

Figure 15. Plot of $\delta^{18}O$ vs. $^{87}Sr/^{86}Sr$ for Hole 735B gabbros. Isotopic composition of seawater is shown for reference. Note the generally large range in $\delta^{18}O$ values yet small range in $^{87}Sr/^{86}Sr$. Lines with steep negative slopes connect mineral separates from Samples 118-735B-4D-2, 18–22 cm; 118-735B-15R-1, 68–72 cm; and 118-735B-1D-2, 80–83 cm (left to right, respectively). Lines with shallow positive slopes connect Samples 118-735B-66R-3, 124–126 cm, and 118-735B-34R-4, 3–4 cm (left to right, respectively). Lines connecting coexisiting phases from all other samples are virtually horizontal.

In addition to their unique radiogenic isotope compositions, these gabbros have unique mineral compositions, both relative to other gabbros in Hole 735B and to gabbros dredged from all other ocean basins (Fig. 16). In particular, they have significantly higher Al/Ti ratios and Cr_2O_3 contents in the clinopyroxenes and higher Cr_2O_3 and NiO contents in the whole rocks. Elthon (1987) attributed high Al_2O_3 contents in gabbros from the Mid-Cayman Rise to crystallization under high-pressure conditions, but this is unrealistic for the Leg 118 gabbros because samples having high Al_2O_3 contents and high Al/Ti ratios occur only tens of meters deeper than samples having low Al_2O_3 contents and low Al/Ti ratios. The combination of relatively radiogenic Sr-isotope ratios with unusual mineral chemistry near the base of the section suggests to us that distinctive magma batches that tapped distinct mantle sources were introduced into the magma chamber through time. This less-abundant magma type had slightly higher $^{87}Sr/^{86}Sr$ and $^{206}Pb/^{204}Pb$ values, but lower $^{143}Nd/^{144}Nd$ values;

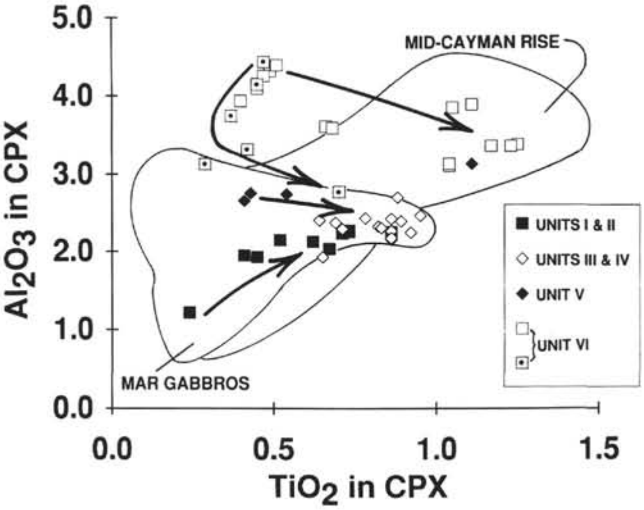

Figure 16. Al_2O_3 vs. TiO_2 in clinopyroxene illustrating the increasing Al/Ti ratio with increasing depth, i.e., from Unit II to Unit VI. Arrows indicate compositional trends with zoning toward the rim. Although clinopyroxene from both Cr-rich gabbros analyzed from Unit VI have high Al/Ti ratios in the cores, zoning trends are different and are shown by different symbols: Sample 118-735B-79R-6, 81–84 cm, open square; Sample 118-735B-85-6, 36–40 cm, square with dot. Shown for comparison are the fields for clinopyroxenes from gabbros dredged from the Mid-Cayman Rise (Elthon, 1987) and from gabbros dredged from the Mid-Atlantic Ridge (Hodges and Papike, 1976; Prinz et al., 1976; Stebbins and Thompson, 1978; Vanko and Batiza, 1982; Bryan et al., 1977; and Clark and Loubat, 1977).

its source must, therefore, have had slightly higher time-integrated Rb/Sr and U/Pb ratios and lower Sm/Nd ratios.

CONCLUSIONS

1. Gabbros from Leg 118, Hole 735B, represent the most complete section through oceanic layer 3 ever recovered from the ocean basins.

2. These gabbros record the cumulate portion of a tholeiitic fractionation trend. Troctolites from lithologic Unit VI were in equilibrium with magmas having Mg numbers of 67 to 69. Olivine gabbros were in equilibrium with more evolved magmas (Mg numbers ranging from 55 to 62); these occur throughout the section recovered, but are most abundant in Units V and VI. In Units I and II, these gabbros are interlayered with significantly more evolved two-pyroxene and FeTi gabbros (whole-rock Mg numbers ranging from 32 to 70). Oxide-rich gabbros constitute approxmately 13% of the core recovered and may be a more common feature of the oceanic crust than previously appreciated.

3. Even in lithologic units where relatively evolved compositions predominate, there remains a continuum of samples having Mg numbers between 80 and 82, suggesting that there was a relatively regular influx of primitive magma into the chamber.

4. Leg 118 gabbros have isotopic compositions that are unique relative to basalts from the SWIR, extending to lower ^{206}Pb/^{204}Pb and higher ^{143}Nd/^{144}Nd values.

5. Although locally highly deformed and altered, whole-rock analyses of gabbros from Hole 735B show that these metamorphic and hydrothermal processes have not altered Sr-, Nd- and Pb-isotope compositions significantly. Sr-isotopic values for whole-rock samples and most plagioclase separates show only limited variation. ^{87}Sr/^{86}Sr values range from 0.7027 to 0.7030. Sr-isotope values in clinopyroxene from the upper half of Hole 735B are higher than coexisting plagioclase (0.7028–0.7037) and probably reflect extensive replacement of clinopyroxene by amphibole. By contrast, O-isotope disequilibrium between coexisting pyroxene and plagioclase pairs from throughout the stratigraphic column indicates that seawater interacted with much of the gabbro section, but at relatively low water/rock ratios and high temperatures.

6. The combination of relatively radiogenic Sr-isotope ratios with unusual mineral chemistry near the base of the section suggests that distinctive magma batches were introduced into the magma chamber through time. The predominant magma type had a ^{87}Sr/^{86}Sr value of 0.7028, a ^{143}Nd/^{144}Nd value of 0.51315, and a ^{206}Pb/^{204}Pb value of 17.4, and occurred throughout the gabbroic column recovered. The second magma type was far less abundant, and occurrence was restricted to the lower portions of Unit VI. Pyroxenes crystallized from this second magma type had significantly higher Cr contents and Al/Ti ratios; Sr- and Pb-isotope data suggest its mantle source also had higher time-integrated Rb/Sr and U/Pb ratios and lower Sm/Nd ratios.

REFERENCES

Anderson, R. N., Zoback, M. D., Hickman, S. H., and Newmark, R. L., 1985. Permeability versus depth in the upper oceanic crust: in-situ measurements in DSDP Hole 504B, Eastern Equatorial Pacific. *J. Geophys. Res.*, 90:3659–3669.

Bryan, W. B., Thompson, G., Frey, F. A., Dickey, J. S., and Roy, S., 1977. Petrology and geochemistry of basement rocks recovered on Leg 37 DSDP. *In* Aumento, F., Melson, W. G., et al., *Init. Repts. DSDP*, 37: Washington (U.S. Govt. Printing Office), 695–704.

Clark, D. B., and Loubat, H., 1977. Mineral analysis from the peridotite-gabbro-basalt complex at Site 334, DSDP Leg 37. *In* Aumento, F., Melson, W. G., et al., *Init. Repts. DSDP*, 37: Washington (U.S. Govt. Printing Office), 847–856.

Cohen, R. S., Evensen, N. M., Hamilton, P. J., and O'Nions, R. K., 1980. U-Pb, Sm-Nd, and Rb-Sr systematics of mid-ocean ridge basalt glasses. *Nature*, 283:149–153.

Cohen, R. S., and O'Nions, R. K., 1982. The lead, neodymium and strontium isotopic structure of ocean ridge basalts. *J. Petrol.*, 23:299–324.

Dupre, B., and Allégre, C. J., 1983. Pb-Sr isotope variation in Indian ocean basalts and mixing phenomena. *Nature*, 303:142–146.

Elthon, D., 1987. Petrology of gabbroic rocks from the Mid-Cayman Rise spreding center. *J. Geophys. Res.*, 92:658–682.

Elthon, D., Lawrence, J. R., Hanson, R. E., and Stern, C., 1984. Modeling of oxygen-isotope data from the Sarmiento ophiolite complex, chile. *In* Gass, I. G., Lippard, S. J., and Shelton, A. W. (Eds.), *Ophiolites and Oceanic Lithosphere:* Oxford (Blackwell Scientific), 185–197.

Goldberg, D., and Becker, K., 1988. Indicators of *in-situ* fracture permeability in oceanic layer 3. *EOS*, 69:1402.

Gregory, R. T., and Criss, R. E., 1986, Isotopic exchange in open and closed systems, *In* Valley, J. W., Taylor, H. P., and O'Neil, J. R. (Eds.), *Stable Isotopes in High Temperature Geological Processes, Reviews, in Mineralogy*. Mineral. Soc. Am., 16:91–128.

Gregory, R. T., and Taylor, H. P., 1981. An oxygen isotope profile in a section of cretaceous oceanic crust, samail ophiolite, oman: evidence for ^{18}O buffering of the oceans by deep (>5 km) seawater-hydrothermal circulation of mid-ocean ridges. *J. Geophys. Res.*, 86:2737–2755.

Hamelin, B., and Allégre, C. J., 1985. Large-scale regional units in the depleted upper mantle revealed by an isotope study of the South-West Indian Ridge. *Nature*, 315:196–199.

Hamelin, B., Dupré, P., and Allégre, C. J., 1985. Pb-Sr-Nd isotopic data of Indian Ocean ridges: new evidence of large-scale mapping of mantle heterogeneities. *Earth Planet. Sci. Lett.*, 67:340–350.

Hart, S. R., and Staudigel, H., 1982. The control of alkalies and uranium in seawater by ocean crust alteration. *Earth Planet. Sci. Lett.*, 58:202–212.

________, 1989. Isotopic characterization and identification of recycled components. *In* Hart, S. R., and Gülen, L. (Eds.), *Crust/Mantle Recycling at Convergence Zones:* Boston (Kluwer Academic), 15–28.

Hedge, C. E., Futa, K., Engel, C. G., and Fisher, R. L., 1979. Rare earth abundances and Rb-Sr systematics of basalts, gabbro, anorthosite and minor granitic rocks from the Indian Ocean ridge system, western Indian ocean. *Contrib. Mineral. Petrol.*, 68:373–376.

Hodges, F. N. and Papike, J. J., 1976. DSDP Site 334: Magmatic cumulates from oceanic layer 3. *J. Geophys. Res.*, 81:4135–4151.

Ito, E., White, W. M., and Gopel, C., 1987. The O, Sr, Nd, and Pb isotope geochemistry of MORB. *Chem. Geol.*, 62:157–176.

Komor, S. C., Elthon, D., and Casey, J. F., 1985. Mineralogical variations in a layered ultramafic cumulate sequence at the North Arm Mountain Massif, Bay of Islands ophiolite, Newfoundland. *J. Geophys. Res.*, 90:7705–7736.

Lister, C.R.B., 1984. The basic physics of water penetration into hotrock. *In* Rona, P., Boström, K., Smith, K., and Laubier, L. (Eds.), *Hydrothermal Processes at Seafloor Spreading Centers:* NATO Conf. Ser. IV, 141–168.

Macdonald, K. C., Fox, P. J., Perran, L. J., Eisen, M. F., Haymon, R. M., Miller, S. P., Carbotte, S. M., Cormier, M.-H., and Shor, A. N., 1988. A new view of the mid-ocean ridge from the behaviour of ridge-axis discontinuities. *Nature*, 335:17–225.

Macdougall, J. D., and Lugmair, G. W., 1986. Sr and Nd isotopes in basalts from the East Pacific Rise: significance for mantle heterogeneity. *Earth Planet. Sci. Lett.*, 77:273–284.

McCulloch, M. T., Gregory, R. T., Wasserburg, G. J., and Taylor, H. P., 1981. Sm-Nd, Rb-Sr and ^{18}O/^{16}O isotopic systematics in an oceanic crustal section: evidence from the Samail ophiolite. *J. Geophys. Res.*, 866:2721–2736.

Michard, A., Montigny, R., and Schlich, R., 1986. Geochemistry of the mantle beneath the Rodriguez triple junction and the South-East Indian Ridge. *Earth Planet. Sci. Lett.*, 78:104–114.

Price, R. C., Kennedy, A. K., Riggs-Sneeringer, M., and Frey, F. A., 1986. Geochemistry of basalts from the indian Ocean triple junction: implications for the generation and evolution of Indian Ocean ridge basalts. *Earth Planet. Sci. Lett.*, 78:379–396.

Prinz., M., Keil, K., Green, J. A., Reid, A. M., Bonatti, E., and Honnorez, J., 1976. Ultramafic and mafic dredge samples from the equatorial Mid-Atlantic Ridge and fracture zones. *J. Geophys. Res.*, 81:4087–4103.

Shipboard Scientific Party, 1989. Site 735. *In* Robinson, P. T., Von Herzen, R. P., et al., *Proc. ODP, Init. Repts.*, 118: College Station, TX (Ocean Drilling Program).

Shirey, S. B., Bender, J. F., and Langmuir, C. H., 1987. Three-component isotopic heterogeneity near the Oceanographer transform, Mid-Atlantic Ridge. *Nature*, 325:217–223.

Stakes, D. S., Taylor, H. P., and Fisher, R. L., 1984. Oxygen-isotope and geochemical characterization of hydrothermal alteration in ophiolite complexes and modern oceanic crust. *In* Gass, I. G., Lippard, S. J., and Shelton, A. W. (Eds.), *Ophiolites and Oceanic Lithosphere:* Oxford (Blackwell Scientific), 199–214.

Stebbins, J., and Thompson, G., 1978. The nature and petrogenesis of intra-oceanic plate alkaline eruptive and plutonic rocks: King's Trough, northeast Atlantic. *J. Volcanol. Geotherm. Res.*, 4:333–361.

Taylor, H. P., 1968. The oxygen isotope geochemistry of igneous rocks. *Contrib. Mineral. Petrol.*, 19:1–71.

Vanko, D. A., and Batiza, R., 1982. Gabbroic rocks from the Mathematician Ridge failed rift. *Nature*, 300:742–744.

White, W. M., Hofmann, A. W., Puchelt, H., 1987. Isotope geochemistry of Pacific Mid-ocean Ridge basalt. *J. Geophys. Res.*, 92:4881–4893.

Whitehead, J. A., Dick, H.J.B., and Schouten, H., 1984. A mechanism for magmatic accretion under spreading centers. *Nature*, 312:146–148.

Date of initial receipt: 27 June 1989
Date of acceptance 21 May 1990
Ms 118B-118

1

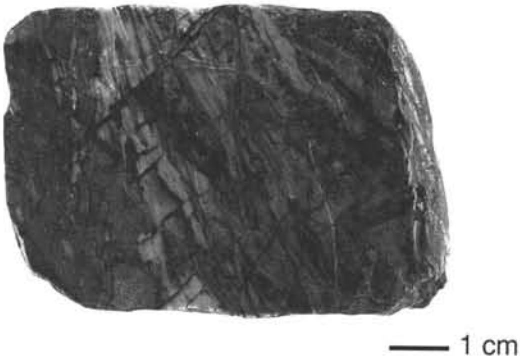

2

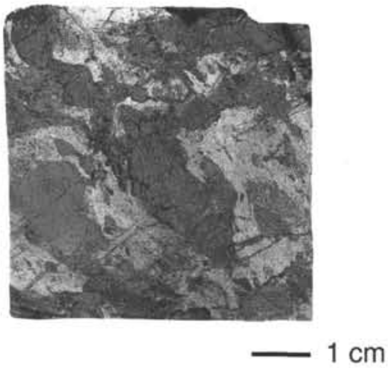

3

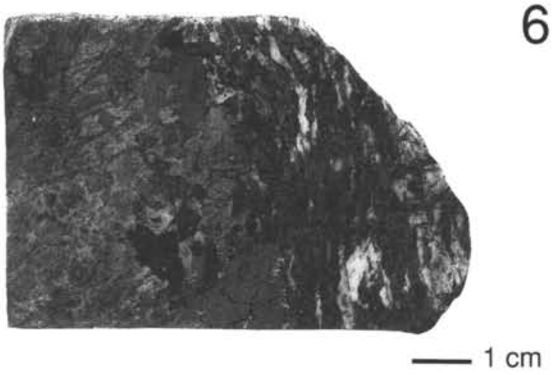

4

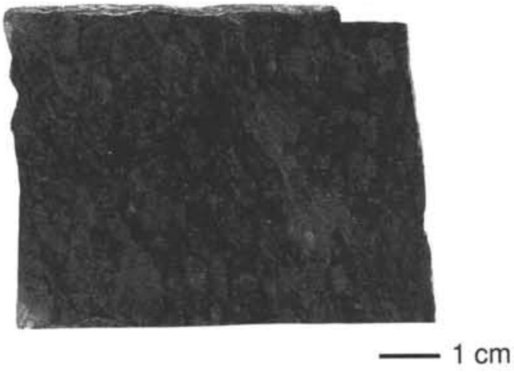

5

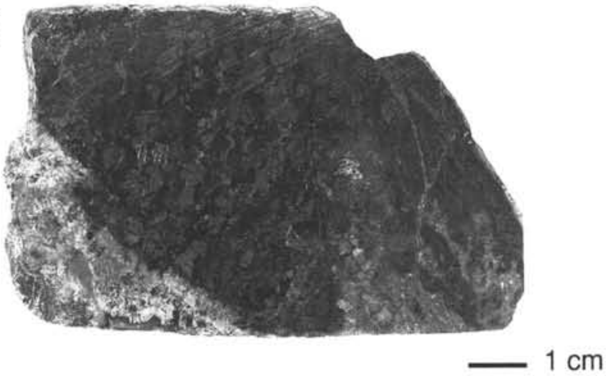

6

Plate 1. **1–6.** Macroscopic features of representative Leg 118 gabbros; see Table 2 for petrographic characteristics.